

# A Multisensor Application of the Electromagnetic Time-Reversal (EMTR) Fault Location Technique

*Alexander Robinson, Cassidy Flynn, and Reza Razzaghi*

**Abstract** – Efficient fault location in power networks is critical in minimizing outage times, though existing methods often require extensive sensor deployment. The time offset maximum derivative (TOMD) method applies electromagnetic time-reversal (EMTR) theory to reduce sensor density but experiences performance degradation with low sensor sampling rates and a high network parameter error. This article extends the TOMD method for multisensor use to address these limitations, introducing the post-TOMD multiplication technique. Two methods of intelligent sensors placement are explored, which use a simple graph-based network representation to efficiently choose sensor locations. Simulation results, using three branched, radial networks, show these methods outperform the single-sensor case and have reduced performance loss at low sampling rates. Moreover, diminishing returns occur when using a large number of sensors, indicating a small set of sensors is usually sufficient for the majority of fault cases.

## 1. Introduction

The operation of transmission and distribution networks can be disrupted by many unexpected events. These include weather-related and man-made disturbances, as well as component failure. Consequently, an efficient method of locating faults is required to minimize supply interruptions and reduce risk associated with these faults. Standard approaches to fault location, such as the use of fault passage indicators, require the installation of many sensing devices in the network. Also, these provide limited fault information, indicating only its relative direction.

The introduction of electromagnetic time reversal (EMTR) in [1] uses the time-reversal invariance of transmission line wave equations to reduce the number of required measurement points to locate a fault. In this process, guessed fault locations are assigned a score, with the maximum over all a priori-guessed fault locations being the predicted fault location. Several scoring metrics have been proposed, including the fault current signal energy [1] and  $L_\infty$  norm [2]. The technique has also been reframed as both a computation of cross-correlation [3] and as a correlation estimator [4]. In

addition, work has been done in [4] and [5] to increase the speed of the EMTR approach. Fundamentally, the EMTR method was improved in [6], with the development of the state-of-the-art time offset maximum derivative (TOMD) approach. This method is robust with variations in fault impedance and network topology [6].

This article aims to address the reduced performance of the TOMD method at low sampling rates (below 1 MHz) and when a high network parameter error is present [6]. This can be achieved by placing a small number of additional sensors in the network. First, a method of collating multiple sensors worth of data (post-TOMD multiplication) is proposed, where the TOMD scores from each sensor are multiplied to produce a final fault location prediction. Second, two potential methods of choosing sensor locations are explored. Both sensor placement methods represent the network as a weighted, undirected graph, using a graph-based structure to choose nodes for sensor placement. The first method minimizes the cumulative distance from all nodes on the graph to the nearest sensor. The second approach groups potential sensor locations with high betweenness centrality (BC) and selects from these the set that minimizes the distance from all nodes to the nearest sensor [7].

Each method was assessed with network simulations at both a moderate and a low sampling rate (1 MHz and 250 kHz, respectively), where typical commercial sensors can reach sampling rates of 330 kHz. The networks were also evaluated across a range of network parameter error values (0% to 15%), which included inserting errors into line length, ground return resistivity, and conductor diameter. These errors are associated with faulty modeling of the network, including adverse weather affecting ground return resistivity and conductor slack causing an incorrect recording of line length.

## 2. Proposed Method of Collating Sensor Data

The current state-of-the-art methodology for EMTR-based fault location methods is the TOMD method [6], which is adapted for this work. The fault-originated transient measured at a sensor can be differentiated to obtain an estimate of the network impulse response, including the corresponding fault path. By convolving this with impulse response signals from a simulation-based preprocessing stage and taking the maximum over a specified time period, a score for each guessed fault location in the network is obtained. The maximum of these scores over all a priori-guessed fault locations corresponds to the predicted fault location.

Manuscript received 19 February 2025.

Alexander Robinson, Cassidy Flynn, and Reza Razzaghi are with Department of Electrical and Computer Systems Engineering, Monash University, Wellington Road, Clayton, Victoria, Australia; e-mail: arob0069@student.monash.edu, cassidy.flynn1@monash.edu, reza.razzaghi@monash.edu.

The proposed post-TOMD multiplication method combines sensor reliability through multiplication on the basis of key principles: a location requires agreement among all sensors to be selected as the fault point, with any single sensor's strong negative assessment significantly reducing the combined score after multiplication. Consequently, locations with moderate confidence scores from all sensors are favored over those with varied assessments. The TOMD score may be expressed as  $\text{TOMD}(s, x, x')$  for some sensor  $s$ , guessed fault location  $x'$ , and true fault location  $x$ . The post-TOMD score is then expressed as

$$\text{pTOMD}(S, x, x') = \prod_{s \in S} \text{TOMD}(s, x, x') \quad (1)$$

the product of individual TOMD scores. Note that  $S$  is the set of sensors placed in the network for data fusion. The final predicted fault location is given by

$$\arg \max_{x' \in X'} [\text{pTOMD}(S, x, x')] \quad (2)$$

where  $X'$  is the set of a priori-guessed fault locations. The performance of this method is evaluated in Sections 4 and 5.

### 3. Proposed Methods of Selecting Sensor Locations

For wave propagation, which forms the theoretical foundation of TOMD, an undirected graph representation is more natural than a directed one. A weighted graph is able to capture the different propagation times of the network, and an undirected graph is useful because it can capture the bidirectionality of transient flow. Let each transformer, junction, and the distribution substation be represented as nodes. The edge weights between these nodes reflect the line lengths between the corresponding network features. An example of such a network is found in Figure 1.

The structure of this graph-based representation can be used to predict sensor placements that together perform well with the previously detailed post-TOMD multiplication method. Crucially, this is done without any network simulations, providing methods that yield identical sensor locations, regardless of network parameter error or sampling rates. Each of the following approaches allows for sensors to be placed at any of the nodes on the graph.

#### 3.1 Distance Minimization

The first method involves minimizing the distance from any node in the network to the nearest placed sensor. This will be referred to as the *distance minimization approach*. Consider a situation in which a set of  $n$  sensors are to be placed in an arbitrary network, represented by an undirected graph with  $N$  nodes, where  $n \leq N$ . Each set of  $n$  nodes is assessed and

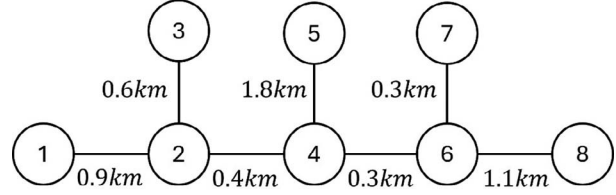


Figure 1. Example of a simple weighted and undirected graph.

assigned a cumulative distance score according to the following

$$\text{distance score} = \sum_{m \in M} \min_{s \in S} d(m, s) \quad (3)$$

where  $M$  is the set of all  $N$  nodes in the graph and  $S$  is the set of  $n$  nodes being assessed;  $d(m, s)$  represents the shortest path distance from node  $m$  to node  $s$ . The set of nodes with the minimum score is chosen as the locations of sensor placement. This method evenly spreads the  $n$  sensors across the weighted graph.

Consider the placement of two sensors on the graph represented in Figure 1 by using distance minimization. The previous algorithm finds that nodes 4 and 5 minimize the distance score metric, obtaining a score of 5 km and placing the sensors at physically distant locations but on neighboring nodes.

#### 3.2 Distance Minimization and the Prioritization of High BC Nodes

The second method is a variation of the previous approach. First, the BC is calculated for each node in the graph [7]. This metric is used to compare how often each node appears on paths between pairs of other graph nodes. The BC of a node  $g$  can be calculated as the following:

$$\text{BC}(g) = \sum_{\substack{s, t \in M \\ s \neq t}} \frac{p_{st}(g)}{P_{st}} \quad (4)$$

where  $M$  is the set of all vertices in the graph,  $p_{st}(g)$  is the number of shortest paths between nodes  $s$  and  $t$  that pass through  $g$ , and  $P_{st}$  is the total number of shortest paths between  $s$  and  $t$ . If  $n$  sensors are to be placed, the  $2n$  nodes with the highest BC values are selected as potential locations. If there are less than  $2n$  nodes in the graph, then all nodes are considered. These candidate positions are subject to the distance minimization process outlined in Section 3.1, using a subset that is large enough to include moderately central positions without defaulting to pure distance minimization (particularly in large networks). In (3),  $M$  is the set of  $2n$  high centrality nodes (or is the set of all nodes, if  $2n \geq N$ , where  $N$  is the total number of nodes). The combination of  $n$  nodes that minimize this score is selected as sensor locations. This is referred to as the *centrality distance minimization approach*. Considering Figure 1 again with two

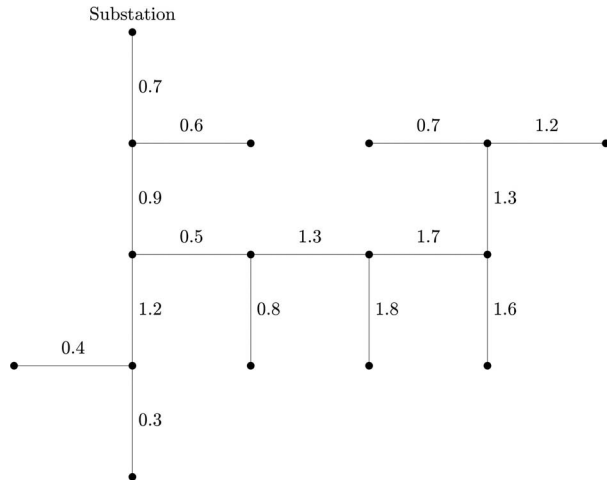


Figure 2. Test Network 1 with a total length of 15 km. Edge labels correspond to distances (in kilometers) between network junctions and endings.

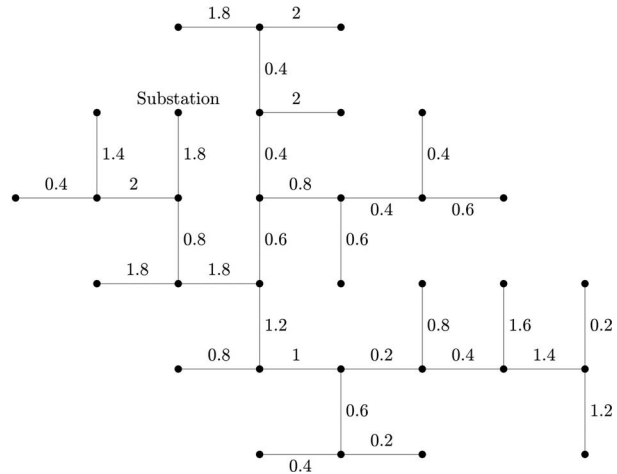


Figure 4. Test Network 3 with a total length of 30 km. Edge labels correspond to distances (in kilometers) between network junctions and endings.

sensors, this placement scheme places sensors on nodes 2 and 6, for a score of 5.3 km. This is worse than the distance minimization score but more evenly places the sensors nodewise on the network.

#### 4. Performance Evaluation Against the Optimal and Single-Sensor Cases

To evaluate the proposed post-TOMD multiplication method in conjunction with graph-based sensor placement techniques, three branched, radial networks were modeled by using EMTP (version 4.2.1) simulation software. Two of the networks had a total length of 15 km (Figures 2 and 3), while the third was a larger 30 km network (Figure 4). Phase to ground faults were placed at 100 m intervals, resulting in 150 fault test

points and 300 test points for the 15 km and 30 km networks, respectively. It was established in [6] that the TOMD method is effective across a broad range of fault impedance values (0  $\Omega$  to 1000  $\Omega$ ). Thus, a fixed fault impedance of 100  $\Omega$  was selected for all test cases. A simulation time step of 200 ns was used, whereby the sensor data were downsampled to the required sampling rate.

Testing was conducted by using a moderate sampling rate of 1 MHz, as well as a lower, practical sampling rate of 250 kHz. At each sampling rate, the success rate was measured against random errors in network parameters (0% to 15%). To measure the success rate of predictions, a 100 m (one fault test point) accuracy threshold was used.

Each junction and terminal in the network was considered as a potential sensor location. The distance minimization approach and the mixed centrality distance minimization approach were both used to select three sensor locations. These were evaluated against the optimal placement of three sensors (determined using exhaustion) that maximized average accuracy for each sampling rate. Three sensors were used in all test cases to maintain low sensor density, consistent with EMTR objectives, while allowing for a meaningful demonstration of sensor aggregation. The diminishing returns of continually increasing sensor counts are explored in Section 5, for a specific case. Crucially, we highlight that distance minimization and centrality distance minimization select consistent sensor placements, regardless of the network parameter error and sampling rate, whereas the optimal placement selects different sensor placements for each sampling rate. Data were combined from the placed sensors by using the proposed post-TOMD multiplication approach. A single-sensor baseline test was also conducted, placing the sensor at each network's substation, as is done in typical single-sensor EMTR-based methods [6].

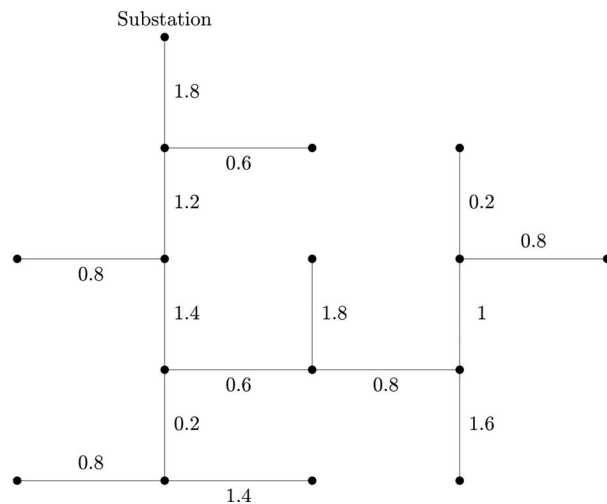


Figure 3. Test Network 2 with a total length of 15 km. Edge labels correspond to distances (in kilometers) between network junctions and endings.

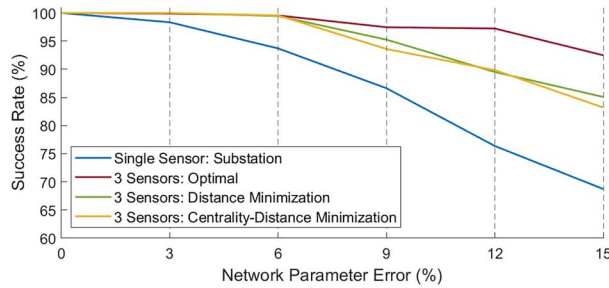


Figure 5. Success rate against increasing parameter error for different methods of sensor placement at a 1 MHz sampling rate. Sensor data are combined by using post-TOMD multiplication.

#### 4.1 Results

Results were averaged across the 15 km and 30 km networks, which can be seen in Figures 5 and 6.

At 1 MHz, the single sensor achieved an average success rate of 87.3%. The optimal placement of three sensors yielded an average success rate of 97.8%, representing an 83% reduction in the misidentification rate compared with the single sensor. The distance minimization approach achieved 94.9%, and the hybrid distance minimization and centrality method produced an average of 94.4%, corresponding to a 60% and 56% reduction of the misidentified faults in the single sensor, respectively. At 250 kHz, the single sensor yielded an 82.9% average success rate. Optimal placement achieved an average of 96.1%, locations chosen with distance minimization yielded 94.0%, and the hybrid approach achieved 92.0%. These correspond to an optimal 77%, distance based 65%, and hybrid based 53% reduction in fault misidentifications compared with the single sensor.

At both sampling rates, the multisensor methods all outperformed the single sensor. Of the two graph-based approaches, at both 1 MHz and 250 kHz, the distance minimization method performed best on average. In both cases, this method achieved an average success rate within 3% of that seen with optimal sensor placement.

The performance for each method decreased as the parameter error increased from 0% to 15%. The relative ranking of methods generally remained consistent, with the two graph-based methods occasionally interchanging positions. At 1 MHz and 0% parameter error, the optimal, distance minimization, centrality distance minimization, and single-sensor cases all achieved average accuracies of 100%, degrading to 92.5%, 85.1%, 83.2%, and 68.7% at 15% error, respectively. Similarly, at 250 kHz, these approaches yielded average accuracies of 100% at 0% network error, falling to 93.2%, 88.6%, 78.0%, and 75.3% at 15% error, respectively.

Moreover, lowering the sampling rate from 1 MHz to 250 kHz saw a decrease of 4.4% in the average accuracy of the single sensor. The graph-based methods of placing sensors, when combined with post-TOMD multiplication, saw decreases of only 0.9% and 2.4% in average accuracy for the distance minimization and centrality distance minimization approaches, respectively. This suggests

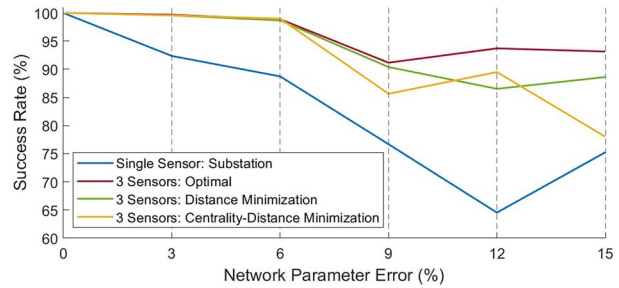


Figure 6. Success rate against increasing parameter error for different methods of sensor placement at a 250 kHz sampling rate. Sensor data are combined by using post-TOMD multiplication.

the distance minimization approach, in particular, is more robust against decreased sampling rates compared with the single sensor.

Note that the optimal sensor locations were chosen by using simulation results to exhaustively determine which three positions, when using post-TOMD multiplication, maximized average accuracy for each sampling rate. Not only is this a computationally expensive process that scales poorly for large networks, but it is also fundamentally liable to overfit results against a specific simulated network parameter error. In comparison, the two placement methods proposed in Sections 3.1 and 3.2 only use the network's graph representation to choose sensor positions and are, hence, robust against overfitting.

#### 5. Evaluation of Performance Gains With Continued Sensor Additions

Further evaluation was conducted on these sensor placement methods with the continued addition of sensors in the 15 km network represented in Figure 2. A sampling rate of 250 kHz was used, while maintaining the same fault impedance, number of fault points, simulation step, and accuracy threshold used in Section 4.

For both graph-based methods introduced in Section 3, the success rate achieved at network parameter error values of 0%, 3%, 6%, 9%, 12%, and 15% was averaged. This was done for an increasing sensor count, with results summarized in Table 1.

For a small number of sensors (less than six, in this case), adding sensors yielded significant performance improvements for both methods. As the number of sensors increased, diminishing returns were obtained. In both cases, using more than six sensors failed to significantly improve the average success rate, which was also the case when placing sensors on all network nodes. This indicates that a handful of well-placed sensors is sufficient to provide network-wide coverage.

#### 6. Conclusion

This study presented a method of combining data from multiple sensors to predict fault locations within a network. This approach applied the method of TOMD,

Table 1. Average success rate of fault location by using graph-based methods of sensor placement, across varying network parameter error values (0% to 15%)<sup>a</sup>

Number of sensors	Distance minimization (%)	Centrality distance minimization (%)
1	80.68	80.68
2	90.29	88.08
3	91.50	90.29
4	90.73	90.73
5	93.38	92.16
6	94.48	94.48
7	93.93	93.93
8	93.93	93.93
16 (sensors on all nodes)	94.59	94.59

<sup>a</sup> Sensor data were combined by using post-TOMD multiplication, with data sampled at 250 kHz. Test Network 1 (Figure 2) was used.

presented in [6], through the process of post-TOMD multiplication. This improved performance at low sampling rates and when there was significant uncertainty in network parameters.

Two computationally efficient methods of multi-sensor placement were explored, using a graph-based representation of the network to select sensor locations. These avoid computationally intensive simulations and prevent overfitting against sampling rates or simulated parameter errors. These methods were tested on three branched, radial networks. Testing used sampling rates of 1 MHz and 250 kHz, with varying network parameter errors (0% to 15%).

The graph-based sensor placement, when used with post-TOMD multiplication, showed performance improvements over the single sensor. Furthermore, these approaches exhibited reduced performance loss with a decrease in the sampling rate from 1 MHz to 250 kHz.

Future work may include further optimization of the post-TOMD multiplication method and testing of additional approaches for multisensor placement.

## 7. References

1. R. Razzaghi, G. Lugrin, H. Manesh, C. Romero, M. Paolone, et al., "An Efficient Method Based on the Electromagnetic Time Reversal to Locate Faults in Power Networks," *IEEE Transactions on Power Delivery*, **28**, 3, July 2013, pp. 1663-1673.
2. S.-Y. He, Y.-Z. Xie, Z.-Y. Wang, F. Rachidi, B.-Y. Liu, et al., "Norm Criteria in the Electromagnetic Time Reversal Technique for Fault Location in Transmission Lines," *IEEE Transactions on Electromagnetic Compatibility*, **59**, 5, October 2018, pp. 1240-1248.
3. Z. Wang, R. Razzaghi, M. Paolone, and F. Rachidi, "Electromagnetic Time Reversal Applied to Fault Location: On the Properties of Back-Injected Signals," *Power Systems Computation Conference*, Dublin, Ireland, June 11-15, 2018, pp. 1504-1510.
4. S. He, A. Cozza, and Y.-Z. Xie, "Electromagnetic Time Reversal as a Correlation Estimator: Improved Metrics and Design Criteria for Fault Location in Power Grids," *IEEE Transactions on Electromagnetic Compatibility*, **62**, 2, April 2020, pp. 598-611.
5. G. Wang, C. Zhuang, and R. Zeng, "An Optimization-Accelerated Electromagnetic Time Reversal-Based Fault Location Method for Power Lines with Branches," *IEEE Transactions on Electromagnetic Compatibility*, **65**, 1, February 2023, pp. 206-215.
6. C. Flynn, R. Razzaghi, and L. L. H. Andrew, "Robust Fault Location Method for Topologically Complex Distribution Networks," *IEEE Transactions on Electromagnetic Compatibility*, **66**, 4, August 2024, pp. 1262-1274.
7. L. C. Freeman, "Centrality in Social Networks Conceptual Clarification," *Social Networks*, **1**, 3, January 1979, pp. 215-239.